IDENTIFYING IMPACT CRATERS RECORDED BY THE APOLLO PASSIVE SEISMIC EXPERIMENT. N. C. Schmerr[1], J. W. Ashley[2], and N. E. Petro[1], [1]NASA-GSFC Greenbelt, MD 20771 USA nicholas.c.schmerr@nasa.gov, noah.e.petro@nasa.gov, [2]Lunar Reconnaissance Orbiter Camera Science Operations Center, Arizona State University Tempe, AZ 85287 USA, james.ashley@ser.asu.edu.

Introduction: From 1969-1977 over 12,000 seismic events were recorded by the Apollo Passive Seismic Experiment (APSE), providing the first-ever seismic observations of the internal structure of another planetary body in the Solar System. However, accurately locating moonquakes is challenging owing to the small number of stations in the Apollo seismic array and the unique character of the lunar seismic wavefield. We strive to improve hypocenter estimations and seismic models of lunar internal structure by identifying fresh craters associated with seismic recordings of meteoroid impacts. Accurate source locations will vastly improve seismic constraints on lunar regolith properties, crustal thickness, seismic attenuation, and mantle velocities.

Background: Approximately 1750 meteoroid impacts were identified by the APSE [1], though only about 30 of these events are seismically located well enough for routine use in inversions for lunar elastic structure [2]. Large uncertainties in lunar travel time inversions arise from the unconstrained location of seismic sources and difficulty in accurately picking scattered P and S-wave travel time arrivals in lunar seismograms [3]. Active source impact experiments of the S-IVB boosters and ascent stage of the Apollo Lunar Modules were used to reduce these uncertainties in early inversions for lunar internal structure, as the exact impact location, mass, velocity, and origin time were provided by telemetry. The active source experiments have been used extensively to calibrate seismic parameters for the natural moonquakes, including meteoroid momentum, seismic amplification, and expected crater size [**Fig. 1**]. The largest impacts recorded by the APSE are expected to have produced craters with diameters of 50-75 m [4].

Craters only a few decades old, down to 1.3 m in diameter, have been recently detected by the Lunar Reconnaissance Orbiter Camera (LROC) by comparing 50-cm to 100-cm per pixel LROC images to Apollo orbital panoramic scans [5]. Fresh craters produce a morphologically sharp feature and high albedo contrast between bright ejecta and dark underlying regolith [**Fig. 2**]. However, challenges in identifying fresh features arise from the varying geometry and photographic artifacts in the older Apollo images. Despite these limitations, visual detection of surface changes on the order of 50-75 m is possible where spatial coverage overlaps between the two datasets.

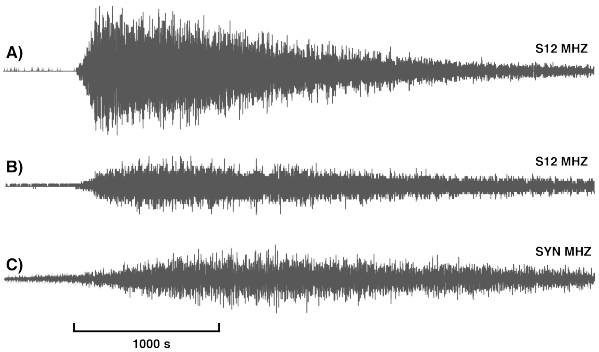

Fig. 1: A) Apollo 12 seismograph of the Apollo 14 S-IVB booster impact on Feb. 4th, 1971. The artificial impact is located at 8.09ºS and 26.02ºW. B) Meteoroid impact recorded by the Apollo 12 station on July 31st, 1972. The impact epicenter is located at approximately 23.4ºN and 7.2ºE. C) 1 Hz reflectivity synthetic seismogram for a 1 km thick lunar regolith with a velocity of 300 m/s [6]. See impact locations in **Fig. 3**.

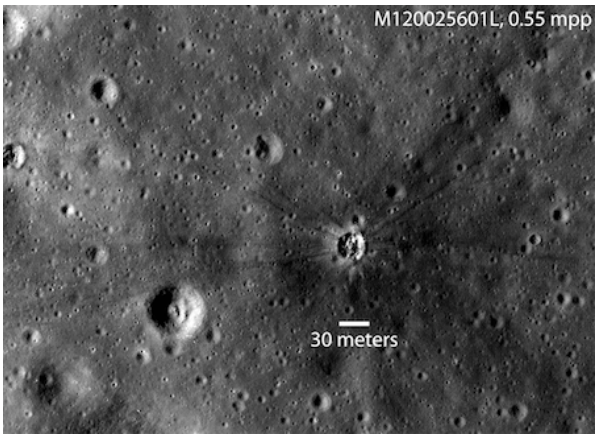

Fig. 2: Example of a recent, morphologically sharp, 35 m diameter crater (near center of image) formed by the artificial impact of the Apollo 14 S-IVB booster. Impact velocity was 2.45 km/s with a mass of 14,106 kg. North is up.

Methods: Fresh craters are recognized by comparing Apollo orbital images to more recent images of the lunar surface, including those taken by the Kaguya Terrain Camera and LROC Narrow Angle Camera. We initially search in the vicinity of well-located meteoroid impacts in an attempt to identify candidate corresponding craters [**Fig. 3**]. Out of the initial catalog of

well-located impacts, at least 12 events fall within regions with coverage from the Apollo panoramic imaging of the lunar surface. Impact events with poorly constrained source locations can also be identified both photogeologically and seismologically, though multiple impacts within the vicinity of the approximate source location may be present [7]. Sources recorded at only one station will fall within a torus; isolating fresh craters in these torii will form the next stage of this study.

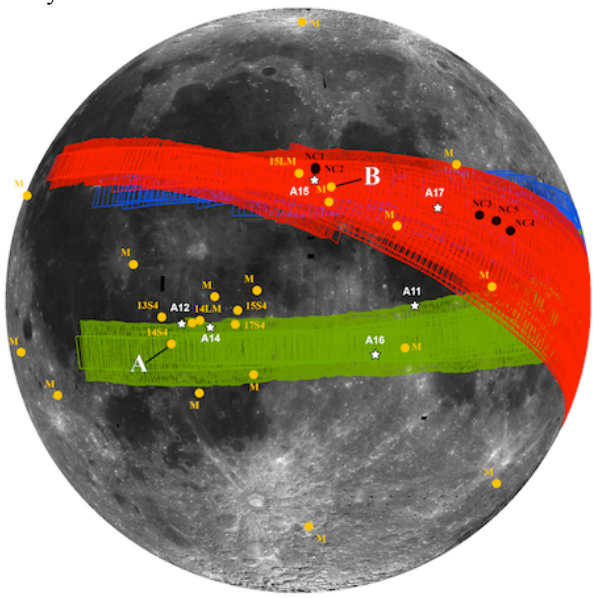

Fig. 3: Panoramic image coverage from Apollo 15 (blue), Apollo 16 (green), and Apollo 17 (red), and seismically determined locations of meteoroid impacts (yellow circles) in the catalog of [8], including the artificial impacts. Apollo landing sites are indicated by white stars. The impacts shown in Fig. 1A and 1B are labeled "A" and "B" respectively. Locations of identified fresh impact craters (NC; black circles) are from [5].

Implications: Once identified, candidate impact events will improve the catalog of moonquakes with the added advantages of crater geometry and precise source locations. Crater size estimates obtained from images links models of crater exhumation and formation processes during the impact [7] with purely seismic spectral estimates of source parameters. The new catalog of source locations will be used to improve travel time estimates for velocity inversions for lunar crustal and mantle structure [9]. Precise epicentral distances are required to evaluate attenuation, scattering, and seismic amplification properties of the regolith [10]. These results will be combined with 3-D waveform propagation of seismic waves [11] scattered and reverberating in the regolith to directly model the lunar seismic wavefield and invert for seismic structure **[Fig. 4]**. Finally, the APSE represents the only in-situ seismic measurements of the natural impact process. Directly tying observations of crater geometry to seismic modeling provides new insight into the cratering process and evolution of the impact craters throughout the Solar System.

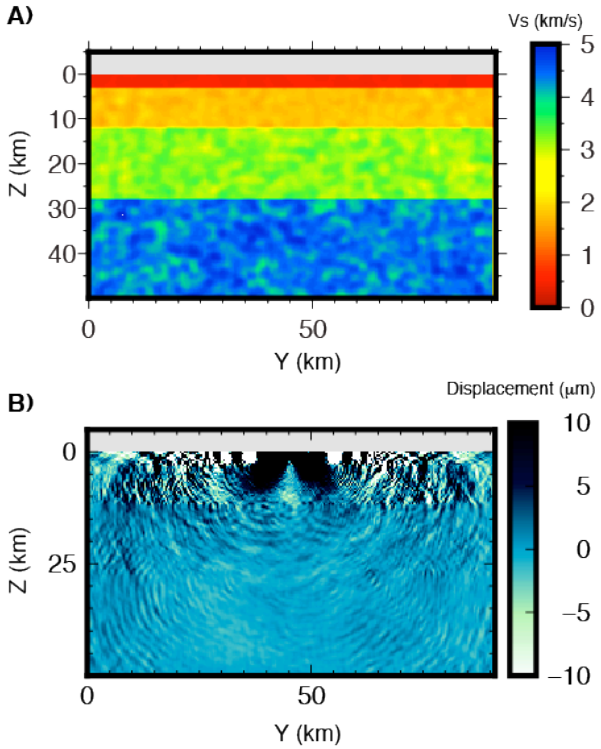

Fig. 4: Vertical cross section through a 3-D finite difference wave propagation simulation [11] adapted for lunar elastic structure. A) Velocity model of [12] with ±5% heterogeneity in a von Karman type media [13]. B) Displacement snapshot at 40 seconds into the simulation. Dominant period is 5 Hz for a 4.0 M_w source implemented at 0 km depth. Grid spacing is 200 m with refinements at 15 km and 1 km depth.

References: [1] ftp://ftp.ig.utexas.edu/pub/PSE/catsrepts [2] Lognonne, P. *et al.* (2003) *Earth Planet Sci Lett* 211, 27. [3] Khan, A. *et al.* (2007) *Geophys J Int* 168, 243. [4] Gudkova, T. V. *et al.* (2011) *Icarus* 211, 1049. [5] Daubar, I. J. *et al.* (2011) *LPS* XLII, Abstract #2232 [6] Fuchs, K. *et al.* (1971) *Geophys J Roy Astron Soc* 23, 417. [7] Oberst, J. *et al.* (1991) *Icarus* 91, 315. [8] Gagnepain-Beyneix, J. *et al.* (2006) *Phys Earth Planet Inter* 159, 140. [9] Nakamura, Y. *et al.* (1970) *Bull Seismol Soc Am* 60, 63. [10] Nakamura, Y. (1976) *Bull Seismol Soc Am* 66, 593. [11] Petersson, N. A. *et al.* (2010) *Lawrence Livermore National Laboratory Technical Report* LLNL-TR-422928, [12] Garcia, R. F. *et al.* (2011) *Phys Earth Planet Inter* 188, 96. [13] Frankel, A. *et al.* (1986) *Journal of Geophysical Research-Solid Earth and Planets* 91, 6465.